Purinergic signaling involved in the cellular response to hypoxia in zebrafish

Anthea Mavridis

A thesis submitted to the University of Ottawa
in partial fulfilment of the requirements for the
Master's degree in Biology

Department of Biology
Faculty of Science
University of Ottawa

Acknowledgements

I would like to begin by thanking my supervisor, Dr. Michael Jonz, for his continued support and guidance throughout my degree. Your leadership and patience have been instrumental not only in my career but in my life as well. I'm looking forward to working with you for a little while longer (you'll never get rid of me).

To my lab mates, thank you for making everyday in the lab a little brighter. Special thank you to Maddy, for passing along all your knowledge and helping me at every step of the way. And to Mohamed, thanks for checking even my most basic calculations and being my BLF (Best Lab Friend). Thank you to my fish and to ACVS for taking such good care of them.

Finally, thank you to my family and friends for making life so much better outside of the lab. I know you won't understand a word of this but will chose to read it anyways, and for that, I am grateful.

.

Abstract

During a hypoxic challenge, the maintenance of cellular function is dependent on an animal's ability to regulate ventilation. Neurochemical signaling in the zebrafish gill initiates reflex hyperventilatory responses at the whole-animal level. Neuroepithelial cells (NECs) are believed to initiate this response by acting on post-synaptic neurons to facilitate reflex hyperventilation via the hindbrain. A number of excitatory and inhibitory neurotransmitters and their receptors have been implicated in hypoxia signalling in the zebrafish gill; however, the current study will focus on purines (ATP and adenosine) as signalling molecules. In the mammalian carotid body, ATP plays a major excitatory role in hypoxia signalling, whereas adenosine is thought to enhance the hypoxic signal. The transgenic zebrafish line, Tg(elavl3:GCaMP6s), expressing a genetically-encoded Ca^{2+} indicator (GCaMP6s) was used to visualize the NEC post-synaptic junction in isolated gill arches, where this contact remains functional. Changes in intracellular Ca^{2+} concentrations ($[Ca^{2+}]_i$) indicated Ca^{2+} activity and were recorded as a proxy for cell excitation. Exposure to the broad-spectrum P2X agonist, ATPγS, post-synaptic $[Ca^{2+}]_i$ increased while exposure to the broad-spectrum antagonist, suramin, caused a decrease in the $[Ca^{2+}]_i$ response to hypoxia. Furthermore, the specific P2X2/3 receptor antagonist, A-317491, caused a decrease in $[Ca^{2+}]_i$ post-synaptically in the gill as well as at the vagus nerve ganglia. These results suggest purinergic involvement in hypoxia signalling in the zebrafish. By contrast, exposure to the broad spectrum P1 receptor antagonist, caffeine, and the specific A2a receptor antagonist, SCH58261, produced no changes in post-synaptic $[Ca^{2+}]_i$ in the gill or at the vagus nerve ganglia. The results of this study suggest that ATP is a major excitatory neurotransmitter acting on post-synaptic P2X2/3 receptors in the initiation of the reflex hyperventilatory response in the zebrafish.

Résumé

Lors d'un test d'hypoxie, le maintien de la fonction cellulaire dépend de la capacité de l'animal à réguler sa ventilation. La signalisation neurochimique dans les branchies du poisson-zèbre déclenche des réponses hyperventilatoires réflexes à l'échelle de l'animal entier. On pense que les cellules neuroépithéliales (NEC) déclenchent cette réponse en agissant sur les neurones post-synaptiques afin de faciliter l'hyperventilation réflexe via le cerveau postérieur. Un certain nombre de neurotransmetteurs excitateurs et inhibiteurs et leurs récepteurs ont été impliqués dans la signalisation de l'hypoxie dans les branchies du poisson-zèbre; cependant, la présente étude se concentrera sur les purines (ATP et adénosine) en tant que molécules de signalisation. Dans le corps carotidien des mammifères, l'ATP joue un rôle excitateur majeur dans la signalisation de l'hypoxie, tandis que l'adénosine est censée renforcer le signal hypoxique. La lignée transgénique de poissons zèbres, Tg(elavl3:GCaMP6s), exprimant un indicateur de Ca^{2+} génétiquement codé (GCaMP6s) a été utilisée pour visualiser la jonction post-synaptique NEC dans des arcs branchiaux isolés, où ce contact reste fonctionnel. Les variations des concentrations intracellulaires de Ca^{2+} ($[Ca^{2+}]_i$) indiquaient l'activité du Ca^{2+} et ont été enregistrées comme indicateur de l'excitation cellulaire. Après exposition à l'agoniste P2X à large spectre, l'ATPγS, le $[Ca^{2+}]_i$ post-synaptique a augmenté, tandis que l'exposition à l'antagoniste à large spectre, la suramine, a entraîné une diminution de la réponse du $[Ca^{2+}]_i$ à l'hypoxie. De plus, l'antagoniste spécifique du récepteur P2X2/3, A-317491, a provoqué une diminution de $[Ca^{2+}]_i$ post-synaptique dans les branchies ainsi que dans les ganglions du nerf vague. Ces résultats suggèrent une implication purinergique dans la signalisation de l'hypoxie chez le poisson-zèbre. En revanche, l'exposition à la caféine, un antagoniste à large spectre des récepteurs P1, et à l'antagoniste spécifique des récepteurs A2a, SCH58261, n'a entraîné aucun changement dans le $[Ca^{2+}]_i$ post-synaptique dans les branchies ou au niveau des ganglions du nerf vague. Les résultats de cette étude suggèrent que l'ATP est un

neurotransmetteur excitateur majeur agissant sur les récepteurs P2 post-synaptiques dans le déclenchement de la réponse hyperventilatoire réflexe chez le poisson-zèbre.

Table of Contents

List of Figures

List of Abbreviations

5-HT – 5-hydroxytryptamine, serotonin

ACh – Acetylcholine

ACVS – Animal Care and Veterinary Services

Ado – Adenosine

ATP – Adenosine triphosphate

$CaCl_2$ – Calcium Chloride

Ca^{2+} - Calcium ion

CB – carotid body

CNS – central nervous system

CO_2 – Carbon dioxide

ChN – Chain Neuron

d.p.f – days post fertilization

eFA – efferent filament artery

ECS – extracellular solution

F/F_0 – relative fluorescence

GFP – green fluorescent protein

hr - hour

HVR – hypoxic ventilatoy response

KCl – potassium chloride

K^+ - potassium ion

min - minute

$MgCl_2$ – magnesium chloride

mm – millimeter

mmHg – millimeters of mercury

mM – millimolar

mRNA – messenger RNA

N_2 – nitrogen gas

NaCl – sodium chloride

NEB – neuroepithelial bodies

NEC – neuroepithelial cells

nAChRs – nicotinic acetylcholine receptors

SV_2 – synaptic vesicle protein 2

O_2 – oxygen gas

ROI – region of interest

Tg – transgenic

μm – micrometer

μM - micromolar

Introduction

Overview

In vertebrates, the ability to sense and respond to low O_2, or hypoxia, is a requirement for organismal development as well as for cellular and tissue homeostasis. Respiratory chemoreceptors are well characterized in mammals and detect changes in the partial pressure (PO_2) of arterial O_2. The glomus, or type I cells, of the mammalian carotid body (CB) and pulmonary neuroepithelial bodies (NEBs) are examples of such cells (Weir *et al*., 2005; Nurse *et al*., 2009; Brouns *et al.,* 2025; Gao *et al.,* 2025). Type I cells have long been considered homologous to the serotonergic neuroepithelial cells (NECs) of fish gills owing to the structural similarities between the carotid body and the first gill arch (Milsom and Burleson, 2007). More recently, it was suggested that pulmonary NEBs are more closely related to fish NECs due to the endodermal origin of both cell types (Hockman *et al*., 2017) and that a novel, cholinergic population of NECs are homologues of type I cells (Reed *et al.,* 2025). In fish, NECs are neuron-like cells located in the adult gill epithelium. They sense low PO_2 (among other physiological parameters such as CO_2/pH) and activate appropriate reflex responses (Jonz and Nurse, 2004, Qin *et al*., 2010, Abdallah *et al.,* 2015). These include the hypoxic ventilatory response (HVR), and changes in heart rate and vascular tone (Perry *et al*., 2009, Burleson *et al*.,1992).

The close evolutionary relationship between O_2 sensitive NECs of fish gills and the chemoreceptors in mammals thus render the zebrafish gills as a powerful comparative tool in understanding the mechanism of hypoxia signalling in vertebrates. Robust methods of chemical screening have already been developed in the zebrafish (Rahbar et al., 2016). In adding to our understanding of ventilation at the cellular level in the zebrafish and how it differs from the control of ventilation in mammals, potential therapeutic targets can be characterized. Their rapid

development may allow for the quick screening of pharmacological agents and characterization of the effects of genetic mutations on O_2 sensing.

NECs were first described containing multiple dense-cored vesicles in the primary lamellae (i.e. filaments) of gills in multiple species by Dunel-Erb *et al*. (1982). They can now be characterized by immunoreactivity with synaptic vesicle protein 2 (SV2) and categorized into two groups by their immunoreactivity with serotonin (5-hydroxytryptamine, 5-HT) or acetylcholine (ACh, Jonz and Nurse, 2003; Reed *et al.,* 2025). The presence of two populations of NECs further strengthens the argument that NECs are homologous to both type I cells and pulmonary NEBs in mammals (Reed *et al*., 2025). The hypoxic response in zebrafish NECs is hypothesized to include the sensing of low O_2, inhibition of background K^+ channels, and cell membrane depolarization, followed by an increase in intracellular Ca^{2+} concentration ($[Ca^{2+}]_i$), which leads to subsequent neurotransmitter release (Jonz *et al*., 2004; Zachar *et al.,* 2017; Reed and Jonz, 2025). The neurotransmitters released presumably act on receptors of post-synaptic neurons that carry the signal to the hindbrain.

Gill Structure and innervation

The gill consists of a complex sensory system that allows for the physiological control of ventilation and gas exchange. The gills of teleosts are composed of four paired gill arches, each supporting two rows of perpendicularly branching filaments. From these filaments extend the secondary lamellae, which are the primary sites of gas exchange. The filaments support both afferent and efferent filament arteries which transport deoxygenated and oxygenated blood, respectively, whereas the lamellae contain a vascular sinus to facilitate gas exchange (Hughes, 1984; Laurent, 1984).

The epithelial layer of the gill consists of a number of cell types, including chemosensory NECs and ionocytes in the filament epithelium and supportive pillar cells and pavement cells of the lamellae (Wilson and Laurent, 2002). The gills are innervated by extrinsic and intrinsic sources. The gills are extrinsically innervated by branches of cranial nerves IX (glossopharyngeal) and X (vagus) which carry sensory and motor fibres between the hindbrain and the gill (Burleson, 2009). Among the sources of intrinsic innervation include the chain neurons (ChNs), superficial proximal neurons and deep proximal neurons that are found extending projections throughout the filaments. Both sources of innervation are found in intimate association with NECs (Jonz and Nurse, 2003).

The two populations of NEC, A-type (cholinergic) and S-Type (serotonergic) are thought to send signals to the hindbrain via two separate excitatory pathways. The A-type NECs are thought to release neurotransmitters (ACh) onto nerve terminals of intrinsic ChNs however, a full attenuation of the response to hypoxia remains to be seen, suggesting other signalling molecules may be involved in mediating the ventilatory response to hypoxia in fish (Reed *et al*., 2025). S-type NECs are thought to directly activate nerve terminals of extrinsic nerve fibres through the release of 5-HT (Reed *et al.,* 2025). Both pathways may lead to the activation of the hypoxic response, and this effect can be inhibited by blocking post-synaptic receptors of both ACh and 5-HT (Reed *et al.,* 2025). A number of other signalling molecules such as ATP and adenosine may act as neuromodulators to advance cellular hypoxia signalling in the zebrafish.

Hypoxia signaling in the CB

In the mammalian CB, it has long been known that a number of neurotransmitters are involved in the transmission of hypoxic signalling. The type I cell response to hypoxia includes a similar cellular cascade to that of the NEC, where hypoxia causes membrane depolarization

followed by neurotransmitter release (López Barneo *et al*., 1988). Among these neurotransmitters are adenosine triphosphate (ATP), adenosine and ACh.

ATP is a key player in mammalian hypoxia signalling and is released from type I cells of the CB to act on purinergic P2X2/3 receptors of petrosal neuron terminals (Zhang *et al.,* 2000; Prasad *et al.,* 2001). In rat vagal nerve afferents, activation of P2X receptors by αβ-MeATP suggested physiological control of respiratory regulation. This activation was inhibited by suramin, a P2X receptor inhibitor (McQueen *et al.,* 1998). Further, hypoxia-evoked ATP release from CB chemoreceptor cells was determined to be dependent on L-type Ca^{2+} channels (Buttigieg and Nurse, 2004). Adenosine, from the break down of ATP via extracellular mechanisms (adenosine equilibrative transporters, (ENT) and ecto-5'- nucleotidases), is also involved in the transmission of hypoxic signalling (Conde and Monteiro*,* 2004). The degree of hypoxia applied (between 2 and 20% O_2) varied adenosine release from rat type I cells (Conde and Monteiro, 2004; Conde *et al*., 2012). In response to moderate hypoxia, it is proposed that ATP is released from vesicles, and the extracellular source of adenosine is the catabolism of ATP (Conde and Monteiro, 2006). Adenosine may enhance the hypoxic signal by acting on purinergic A2a receptors of type I cells (reviewed by Nurse, 2014). Taken together, the excitatory effects of adenosine via A2a receptors and ATP via P2X receptors indicate that they are primary transmitters of the hypoxic signal in mammals.

Early studies identified ACh as an important transmitter of the hypoxic response in mammals. It was initially favoured as a neurotransmitter released during hypoxia and mediated by nicotinic acetylcholine receptors (nAChRs) of petrosal neurons (Zhong and Nurse, 1997)). This excitation by hypoxia could be partially blocked by the application of hexamethonium and induced by application of nicotine (Zhong and Nurse, 1997). It was later found that ACh is co-released with ATP during a hypoxic event to stimulate nAChRs and P2X2 receptors of post-synaptic

neurons to initiate ventilation (Zhang *et al.,* 2000). ATP is frequently co-released with neurotransmitters including ACh in both the central and peripheral nervous systems (Burnstock, 2020).

Hypoxia signaling in the gills of teleosts

This mechanism of hypoxia signalling is also plausible in the adult zebrafish gill where many neurotransmitter and receptor candidates have been suggested, including dopaminergic, cholinergic, serotonergic and purinergic receptors. In the zebrafish, at the level of the NEC-ChN junction, dopamine was determined to have neuromodulatory effects on ventilation, while ACh has been found to have excitatory effects on ventilation (Reed and Jonz, 2025; Reed *et al*., 2025). Furthermore, it has been shown that the Ca^{2+} response in ChNs is dependent on the activation of NECs by hypoxia (Reed and Jonz, 2025). In gills in which synaptic contact between NECs and ChNs was chemically or physically ablated, the hypoxic response was completely abolished in ChNs (Reed and Jonz, 2025). This suggests that the ChN acts as the post-synaptic element that carries the hypoxic signal to the hind brain by way of the vagus nerve.

The current study will focus on purinergic signalling molecules as neurotransmitters including ATP and adenosine. Purinergic receptors can be subdivided into two categories, P1 and P2. P1 receptors are G-protein-coupled receptors that are selective for adenosine and have four known subtypes, A1, A2a, A2b and A3. P2 ATP receptors are further divided into the ligand-gated ion channels, P2X1-7, and the G-protein-coupled receptors, P2Y1-12 (reviewed by Burnstock, 2018). Adenosine receptors are coupled to adenylate cyclase, through which adenosine has an inhibitory downstream effect by binding to A1/3 or a stimulatory downstream effect by binding to A2a/b (Reshkin *et al*., 2000). ATP receptors consist of either homomultimers or heteromultimers that form a trimer ion channel (Nicke *et al.,* 1998). While it is clear that ATP and adenosine

contribute to the hypoxic response in mammals, physiological evidence for purinergic activity in the zebrafish remains less studied.

Using methods of chemical screening, it was found that the hyperventilation response to hypoxia involves both purinergic and adenosine signalling in the zebrafish (Rabhar *et al.,* 2016, Coe *et al.,* 2017). A number of chemicals including suramin, a broad spectrum P2X antagonist, and A-317491 and PPADS, specific P2X3 and P2X2/3 receptor antagonists respectively, inhibited the hyperventilation response to hypoxia; whereas the broad-spectrum agonist, ATPγS elicited a hyperventilatory response similar to the response observed during hypoxic exposure (Rahbar *et al*., 2016; Coe *et al.,* 2017).

Furthermore, caffeine, a broad-spectrum adenosine receptor antagonist and SCH58261, a specific A2a receptor antagonist both inhibited the hyperventilatory response to hypoxia in zebrafish, implicating A2a in the transmission of the hypoxic response (Coe *et al.,* 2017). Moreover, P2X3 receptors colocalized with serotonergic NECs in the gill filaments of developing zebrafish (Jonz and Nurse, 2003; Rahbar *et al.,* 2016). These findings suggest a role for both the P2X2/3 and A2a receptors in mediating the transmission of the hypoxic response in the adult zebrafish gill

Research goals

The primary goal of this study was to determine the specific purinergic and adenosine receptors involved in the transmission of the hypoxic response in the adult zebrafish. We hypothesized that during the cellular response to hypoxia, ATP and adenosine will facilitate hypoxia signaling through P2X2/3 purinergic receptors and A2a adenosine receptors. The first objective in this study was to obtain physiological evidence for the specific receptor types involved

in hypoxia signalling at the NEC-ChN synapse in the gill through the use of agonists and antagonists that target ATP and adenosine receptors while recording Ca^{2+} activity in ChNs. The second objective was to use a similar pharmacological approach, but record Ca^{2+} activity at the level of the vagal sensory ganglia. Implicating ATP and adenosine as neurotransmitters involved in hypoxia signalling both at the level of the gill and vagus nerve provide further evidence that sensory information from the NEC is sent to the hindbrain via the ChN and vagal sensory ganglia to initiate the reflex hyperventilatory response.

The primary goals were evaluated using *ex vivo* Ca^{2+}-imaging with a previously-established transgenic zebrafish line having a genetically-encoded Ca^{2+} indicator driven by the expression of a pan-neuronal marker Tg(*elavl3*:GCaMP6s) (Dunn *et al*., 2016; Reed and Jonz, 2025). The indicator consists of a green fluorescent protein (GFP) molecule, the Ca^{2+}-binding protein, calmodulin (CaM) and the M13 peptide of the myosin light chain kinase protein. In this model, Ca^{2+} interacts with CaM which causes a confirmational change that allows CaM and M13 to bind resulting in a subsequent conformational change that increases the intensity of GFP fluorescence, indicating changes in $[Ca^{2+}]_i$ (Nakai et al., 2001).

In the present study, relative changes in $[Ca^{2+}]_i$ in ChNs and vagus nerve ganglia were used as an indicator of cell excitation and recorded in relative fluorescence. Whole gill arches, as well as larvae at 14-21 days post fertilization (d.p.f), were exposed to agonists and antagonists of both ATP and adenosine receptors and relative changes in fluorescence were recorded. We proposed that ATP and adenosine will be released during a hypoxic event to act post-synaptically in order to facilitate hypoxia signalling towards the hindbrain and initiate reflex hyperventilatory responses.

Experimental design

Animals

Tg(*elavl3*:H2B-GCaMP6s) adult zebrafish (*Danio rerio*) were housed at the University of Ottawa in the Laboratory for the Physiology and Genetics of Aquatic Organisms and cared for by Animal Care and Animal Services (ACVS). Fish were maintained in a closed system of dechloraminated City of Ottawa water at 28.5˚C, kept on a light:dark cycle of 14h:10h and fed once daily (Westerfield, 2000). When needed, embryos were collected as previously described by Westerfield (2000), using standard breeding methods, and transferred to Petri dishes containing embryo medium (3 mL methylene blue diluted in 1 L system water). Embryos were screened for fluorescence of GFP at 24 h post-fertilization. All procedures were conducted using protocol BL-3666 and in accordance with the guidelines established by the Canadian Council for Animal Care (CCAC).

Calcium imaging

Whole gill baskets were removed from adult zebrafish (2-4 months post-fertilization) euthanized by concussion and decapitation. Separated gill arches were placed in a Petri dish fitted with a bath chamber (Warner Instruments, cat no. 64-0388) under a tissue anchor (cat. no. 64-0251, Warner Instruments) to prevent movement from the flow of solution. In the case where larvae were used, single live specimens between 14 and 21 d.p.f. were placed laterally in the bath chamber and pinned in place with two tungsten wire pins (Scientific Instrument Services, Inc. cat no. W406) placed in the larva at the eye and through the body, caudal to the swim bladder. Larvae were used beginning at 14 d.p.f as at this stage, gill NECs are fully innervated (by 7 d.p.f.; Jonz and Nurse, 2005) and the gills become a functional gas exchange organ (Rombough, 2002). No change was observed in Ca^{2+} responses between 14 and 21 d.p.f. The bath was lined with Sylgard 184 (Fisher

Scientific, cat no. NC9644388) to ease pinning. Tricaine methanesulfonate (MS-222) at 0.04% was added to all solutions for larval anesthetization and buffered with $NaHCO_3$.

The bath chamber held approximately 800 µL of solution. Polyethylene tubing was used in superfusion and was non-porous to assure no transfer of O_2 to the superfusate (Tygon, Fisher Scientific, cat no. 141691A). The chamber was first perfused with a normoxic extracellular solution (ECS; 120 mM NaCl, 5 mM KCl, 2.5 mM $CaCl_2$, 2 mM $MgCl_2$, 10 mM HEPES, 10 mM glucose at pH 7.8) at a rate of 4ml/min, where a baseline of fluorescence was collected in each recording. Following this, hypoxic ECS was applied to the bath. Solution was made hypoxic by bubbling with N_2 to displace the O_2 until the PO_2 reached approximately 35 mmHg. In a control recording, the hypoxic perfusion occurred three times followed by normoxic solution in between, to ensure recovery of the cell as well as ensuring that the response remained the same magnitude over time. In the case where the recording included a chemical application, if the drug used was a purinergic antagonist, it was applied during hypoxia when endogenous ATP/Ado is presumably released. If it was a purinergic agonist, it was applied during normoxia to activate the purinergic receptors.

Fluorescence intensity was recorded using NIS-elements software connected to either a Nikon Ni-U fluorescence microscope fitted with a Lumencor LED light or a Nikon Eclipse FN1 fitted with a Lamba DG-5 wavelength changer (Sutter Instruments). Video recordings as well as the time measurement of relative fluorescence units (F/F_0) of a specific region of interest (ROI) or cell was recorded using an EMCCD detector (Ni-U) or a CCD detector (FN1). The ROIs were centered around the fluorescent nucleus of a ChN (determined based on morphology described in Reed and Jonz, (2025), as well as placed over an area of inactivity for calculation of the

background fluorescenc. GFP was detected using a 40× water emersion objective lens (Nikon, Japan). Sampling occurred once every 1-2 s.

Drugs

All drugs were obtained from Millipore Sigma. Suramin, a broad-spectrum purinergic P2X antagonist (suramin sodium salt, cat no. S2671), was dissolved for a final concentration of 200 μM in ECS. Adenosine 5'-triphosphate (ATPγS), a broad-spectrum P2X agonist (cat. no. A1388), was first dissolved in dimethyl sulfoxide (DMSO, at a final concentration of 0.5%) for a final concentration of ATPγS of 300-500 μM in ECS. A-317491, the specific P2X2/3 inhibitor (A-317491 sodium salt hydrate, A2797), was dissolved first in DMSO (0.5%) for a final concentration of 100-400 μM. Caffeine, the broad-spectrum adenosine receptor antagonist (cat. no. 205548) was dissolved in H_2O for a final concentration of 300 μM. SCH 58261 the A2a antagonist (cat. no. S4568) was dissolved first in DMSO (0.5%) for a final concentration of 10 μM.

As some drugs were first dissolved in 0.5% DMSO, control experiments included exposures to 0.5% DMSO in ECS to determine whether DMSO produced any effect. ChN recordings demonstrated no significant changes in $[Ca^{2+}]_i$ in response to 0.5% DMS0 in ECS (Appendix A, Friedman test with Dunn's multiple comparisons, P=0.7402, n=6). Due to limited supply of ATPγS, this reagent was bath-applied and washed out with the superfusion system. Control experiments for ATPγS included manually pipetting ECS into the dish with a Pasteur pipette to ensure that there were no changes in fluorescence from manual bath pipetting. No significant increase in the $[Ca^{2+}]_i$ response to hypoxia in ChNs was demonstrated between the baseline and manual application of ECS with 0.5% DMSO (Appendix A, Friedman test with Dunn's multiple comparisons, P=0.0055, n=6).

Statistical analysis

The reported sample size (*n*) refers to the number of individual cells or ganglia in whole-gill or larval recordings, respectively. For whole-gill recordings, 82 cells were obtained from 65 adult zebrafish and multiple gill arches were assessed per fish. For larval recordings, 24 ganglia (epibranchial and nodose ganglia) were obtained from 14 fish. Baseline fluorescence was used to compare changes in fluorescence in each recording and was calculated as the average fluorescence intensity of a cell in 1 min of recording in normoxia. Ca^{2+} response values were acquired by taking the average of 30 s of relative fluorescence units over the peak of the response. For all recordings, fluorescence values were divided by the baseline to assess changes in fluorescence intensity over time for the duration of individual recordings.

Statistical analysis for both gill and larval recordings was carried out with GraphPad Prism v9.5.1 (GraphPad Software Inc., San Diego, CA, USA). A Friedman test with Dunn's multiple comparisons was used for paired tests with three treatments; the Wilcoxon matched-pairs signed rank test was used for paired tests with two treatments; and the Mann-Whitney test was used for unpaired tests. The dose-response curve was expressed as percent inhibition. For estimation of IC_{50}, a line through the origin at zero was fit to the data using [Inhibitor] vs. response – variable slope (four parameters) and data points were fit following the equation y = bottom + (Top-bottom)/$(1+IC_{50}/X^{HillSlope})$. All data were expressed as mean with +/- standard deviation (SD).

Results

To investigate a potential excitatory role for ATP and adenosine as signalling molecules facilitating the ventilatory response to hypoxia in the zebrafish, Ca^{2+}-imaging protocols were adapted from Reed and Jonz (2025) and Reed *et al.* (2025) (Fig. 1A-D). Gill arches were exposed to three successive bouts of hypoxia and changes in $[Ca^{2+}]_i$ in ChNs were recorded (Fig. 1E). Hypoxia produced an increase in $[Ca^{2+}]_i$ and there was no significant difference in relative fluorescence between each hypoxia exposure indicating no changes in Ca^{2+} activity in ChNs between bouts (Fig. 1F, P=0.9563, n=6).

The Ca^{2+} response to hypoxia in chain neurons occurred via P2X2/3 receptors

In order to implicate the potential involvement of purinergic receptors in hypoxia signalling in the zebrafish, broad spectrum reagents targeting the P2 category of ATP receptors were used to either elicit or inhibit the ChN response to hypoxia. In order to assess a role or ATP as an excitatory signalling molecule in the ChN response to hypoxia, ATPγS, a non-hydrolysable ATP analog was first used. Exogenous application of 300-500 μM ATPγS, increased ChN relative fluorescence by 47.5% from the baseline (Fig. 2A, B). This indicated a significant increase in Ca^{2+} activity in ChNs when ATPγS was applied in the absence of hypoxia (P=0.0002, n=11).

As a next step, suramin, a broad-spectrum purinergic antagonist, was combined with hypoxia and the ChN response to hypoxia was assessed. Suramin induced a marked decrease in $[Ca^{2+}]_i$ in ChNs during hypoxic stimulation (Fig. 2C, D). When 200 μM suramin was applied to the bath chamber during hypoxia, ChN relative fluorescence decreased by approximately 41% in comparison to the first hypoxia exposure (P=0.0281, n=6). This indicated that endogenous ATP activity on ChNs was inhibited by suramin.

Figure 1. Schematic representation of the *ex vivo* gill preparation and experimental protocol for Ca^{2+}-imaging. (A,B) An intact gill basket is shown post-dissection, and an isolated gill arch is shown in with a dashed box to represent the filament portion viewed in C and D. Gill arches are labeled 1-4 in A, scale bar represents 0.5 mm and applies to panel B. (C) A cartoon depiction of the innervation of the neuroepithelial cell-chain neuron (NEC-ChN) synapse. The left panel shows the efferent aspect of a gill filament depicting NECs in the distal portion and ChNs running just inferior to the NECs. The right panel shows a 90˚ rotation of the filament showing the proposed synaptic contact between NECs and ChNs. (D) A schematic representation of the Ca^{2+}-imaging protocol is shown with a close-up of a gill filament (dashed box from B) held in the bath chamber. The gill filament is shown with two fluorescing ChNs and the dashed line is for visualization of the shape of the lamellae on one side. L= lamella, eFA= efferent filament artery, F = filament, scale bar = 40 μm. (E) A Ca^{2+}-imaging trace is shown demonstrating the post-synaptic ChN responses to three isolated hypoxia exposures (time of application is represented with bars across the top of the trace). The trace demonstrates the change in $[Ca^{2+}]_i$ for each exposure. Scale indicates time (min) and relative changes in fluorescence (F/F_0). (F) Summary data with mean relative fluorescence +/- SD associated with each hypoxic exposure in E. No significant difference was observed between each hypoxic exposure. (Friedman test with Dunn's multiple comparisons, p=0.9563, n=6).

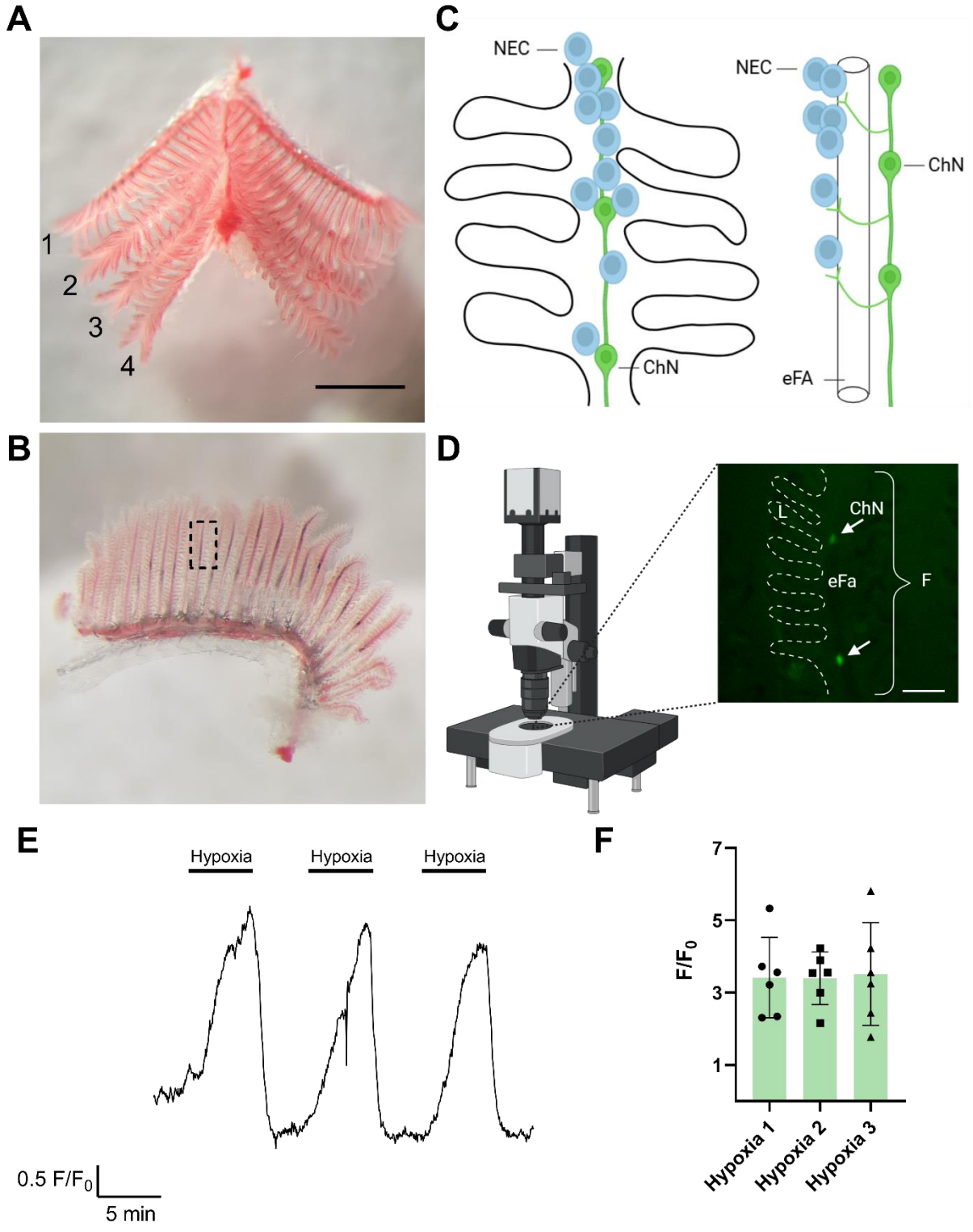
A
1
2
3
4
B
C
NEC
NEC
ChN
ChN
eFA
D
L
ChN
eFa
F
E
Hypoxia
Hypoxia
Hypoxia
0.5 F/F0
5 min
F
F/F0
7
5
3
1
Hypoxia 1
Hypoxia 2
Hypoxia 3

Figure 1

Figure 2. ATPγS, increased $[Ca^{2+}]_i$ in chain neurons, whereas suramin reduced the hypoxia-induced increase in $[Ca^{2+}]_i$. (A) A Ca^{2+}-imaging trace demonstrates an increase in $[Ca^{2+}]_i$ by 47.5% from the baseline in the presence of 300-500μM ATPγS. The cell was also exposed to hypoxia for reference. (B) Summary data demonstrating the increase in mean relative fluorescence +/- SD associated with ATPγS exposure in A (Friedman test with Dunn's multiple comparisons, P=0.0002, n=10), and no statistical significance was observed between normoxia and recovery (Friedman test with Dunn's multiple comparisons, P=0.5391, n=10). (C) A Ca^{2+}-imaging trace demonstrates a 41% decrease in $[Ca^{2+}]_i$ during hypoxia in the presence of 200 μM suramin (SUR) compared to the initial hypoxic response. Scale indicates time (min) and relative changes in fluorescence (F/F_0). (D) Summary data demonstrating mean relative fluorescence +/- SD associated with each exposure in C. Addition of 200 μM SUR significantly reduced the Ca^{2+} response to hypoxia (Friedman test with Dunn's multiple comparisons, P=0.0281, n=6). The response was fully recovered after treatments (Friedman test with Dunn's multiple comparisons, P=0.2498)

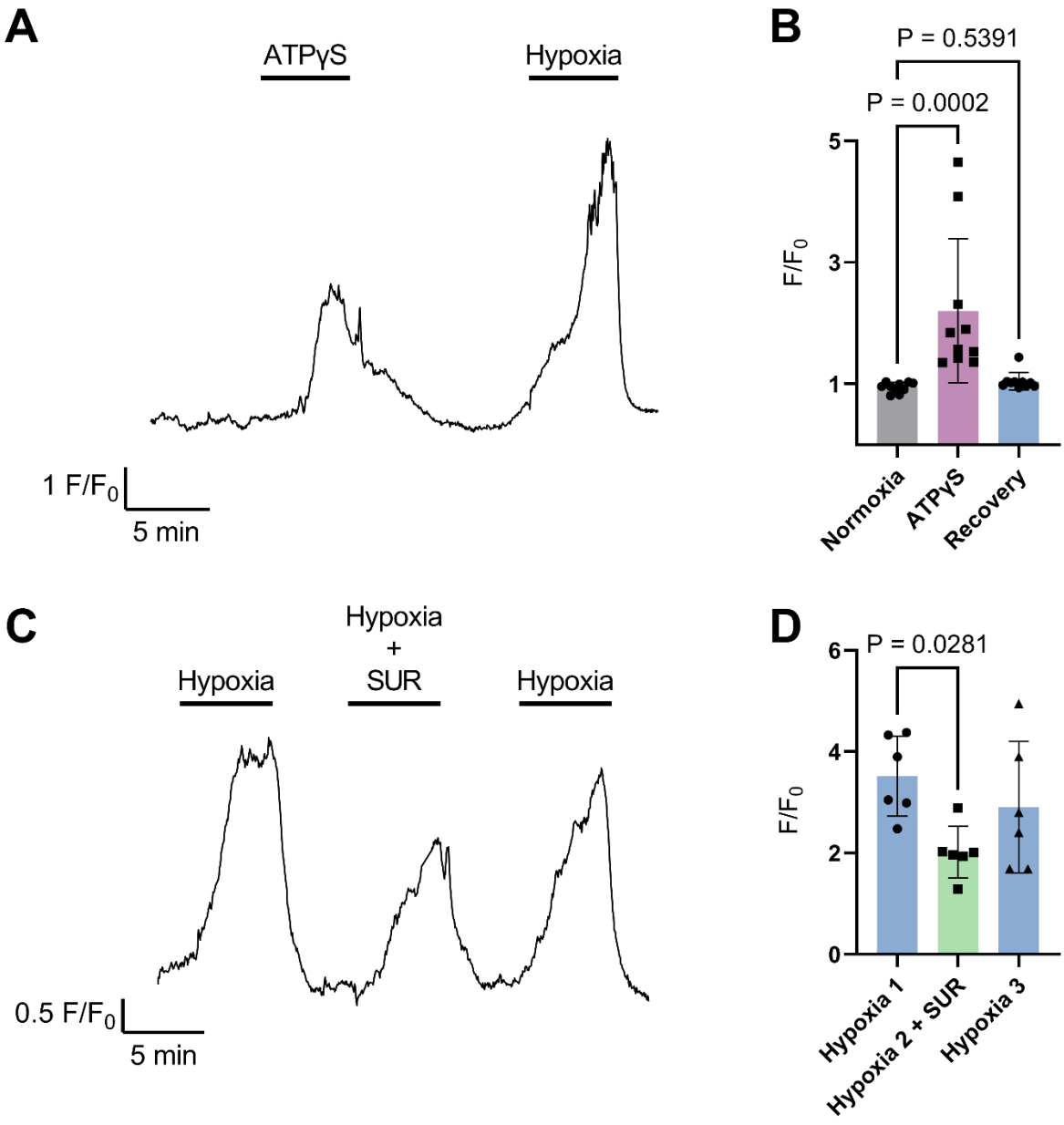
A
ATPγS
Hypoxia
1 F/F0
5 min
B
P = 0.5391
P = 0.0002
F/F0
Normoxia
ATPγS
Recovery
C
Hypoxia
Hypoxia + SUR
Hypoxia
0.5 F/F0
5 min
D
P = 0.0281
F/F0
Hypoxia 1
Hypoxia 2 + SUR
Hypoxia 3

Figure 2

To further implicate a specific purinergic receptor subtype in the ChN response to hypoxia, the specific P2X2/3 antagonist, A-317491 was used. Inhibition of P2X2/3 receptors with A-317419 reduced the ChN response to hypoxia in a dose-dependent manner (Fig. 3A, B). In the presence of A-31749, at concentrations between 100-400 μM, the ChN response to hypoxia was increasingly inhibited as the concentration of A-317491 increased. The ChN response to hypoxia was significantly reduced by 47.2% at 400μM (Wilcoxon matched-pairs signed rank test, P=0.0039 n=9), by 35.3% at 300μM (P=0.0313, n=6), by 19.0% at 200μM (P=0.0313, n=6), and by 11.0% at 100μM (P=0.0313, n=6). The percent inhibition of the cellular hypoxic response between hypoxia exposure and hypoxia with A-317491 was then plotted to determine the IC_{50} of A-317491 which was approximately 400 μM (Fig. 3C).

ATP and ACh contribute to hypoxia signalling at the level of the NEC

During the hypoxic response in the zebrafish gill, ACh is released from NECs to act on nAChRs of post-synaptic ChNs (Reed *et al.,* 2025). In the present study, it was found that ATP, presumably released from NECs, acted on post-synaptic P2X2/3 receptors of ChNs. Given that both of these neurotransmitters were determined to be released individually, we next aimed to create an argument for their co-transmission, a mechanism also noted in the mammalian CB where ATP and ACh are released together from type I cells to act post-synaptically (Zhong and Nurse, 1997)

Inhibition of nAChRs by hexamethonium was previously determined by Reed *et al.,* (2025) as having an IC_{50} of 79.4 μM. In the current study, 100 μM hexamethonium (HEX) and 300 μM A-317491 were applied simultaneously with hypoxia to inhibit both nAChRs and P2X2/3 receptors on post-synaptic ChNs. The result was an increased inhibition of the ChN response to hypoxia in response to HEX with A-317491 when compared to HEX and A-317491 applied alone

Figure 3. The specific P2X2/3 antagonist, A-317491, reduced the hypoxia-induced change in $[Ca^{2+}]_i$ in a dose dependent manner. (A) Ca^{2+}-imaging traces demonstrate relative changes in fluorescence when gills were exposed to hypoxia and to hypoxia with varying concentrations of A-317491. The $[Ca^{2+}]_i$ response to hypoxia was reduced in the presence of increasing concentrations of A-317491 from 100-400 μM. Scale indicates time (min) and relative changes in fluorescence (F/F_0) and applies to all traces. (B) Summary data of the mean relative fluorescence +/- SD associated with each concentration. The hypoxic response was significantly reduced by 47.2% at 400 μM (Wilcoxon test, P=0.0039, n=10), by 35.3% at 300 μM (Wilcoxon test, P=0.0313, n=9), by 19.0% at 200 μM (Wilcoxon test, P=0.0313, n=6), and by 11.0% at 100 μM (Wilcoxon test, P=0.0313, n=6). Error bars represent SD. Percent inhibition was calculated between hypoxia and hypoxia with A-317491 and plotted against concentration of A-317491 in (C). A non-linear curve was fit using an [inhibitor] vs. response – variable slope (four parameters) model with least squares fit. The IC_{50} of A-317491 was approximately 400 μM.

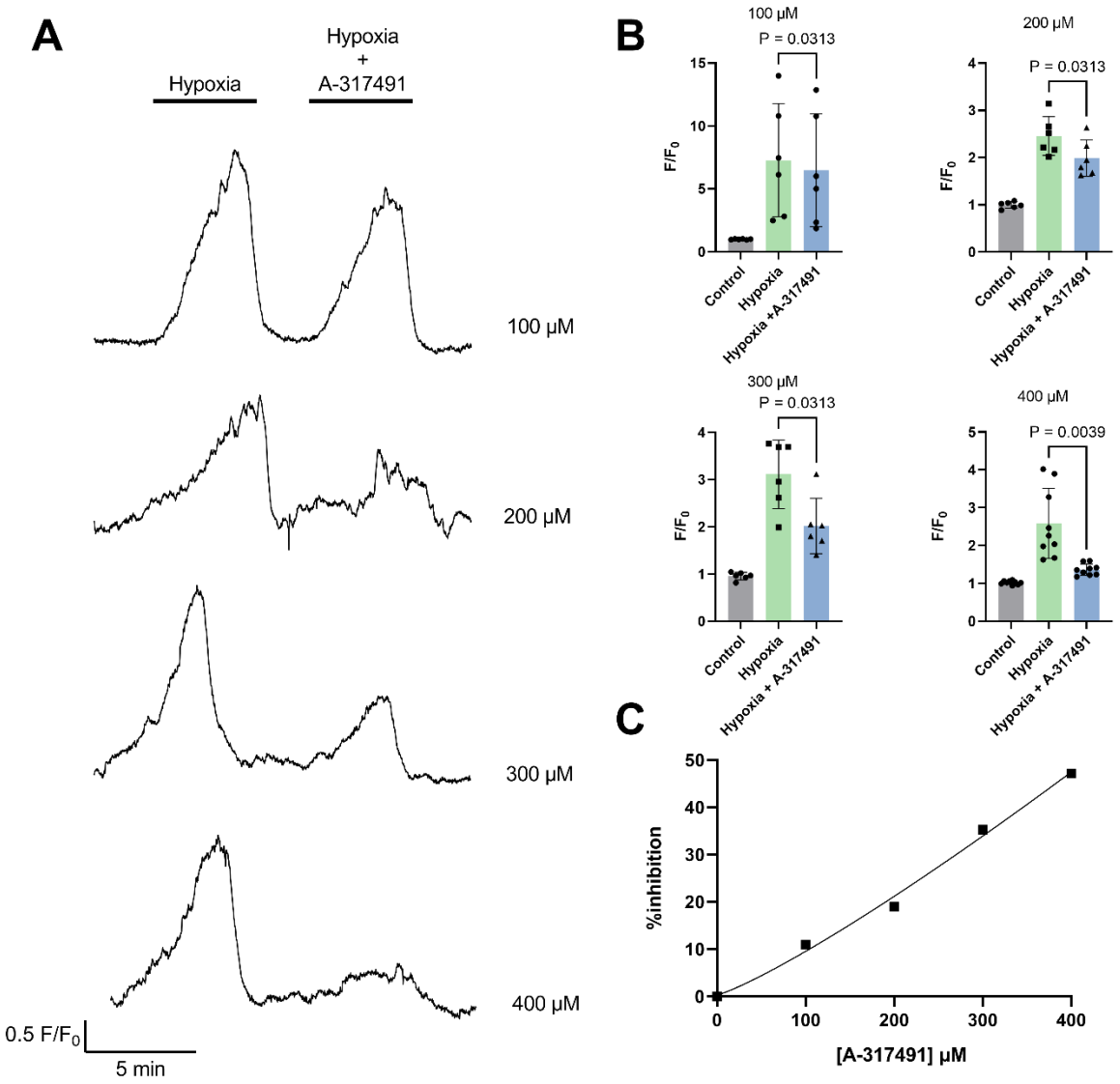
A
Hypoxia
Hypoxia + A-317491
100 µM
200 µM
300 µM
400 µM
0.5 F/F0
5 min
B
100 µM
P = 0.0313
200 µM
P = 0.0313
300 µM
P = 0.0313
400 µM
P = 0.0039
F/F0
Control
Hypoxia
Hypoxia + A-317491
C
%inhibition
[A-317491] µM

Figure 3

Figure 4. Adenosine triphosphate and acetylcholine contribute to hypoxia signaling at the NEC-ChN synapse. (A) A Ca^{2+}-imaging trace showing a depression in the change in $[Ca^{2+}]_i$ in ChNs at the EC_{50} of hexamethonium (HEX, 100 μM). (B) A Ca^{2+}-imaging trace demonstrating a decrease in $[Ca^{2+}]_i$ in the presence of 300 μM A-317491 and 100 μM HEX applied simultaneously during hypoxia exposure. Scale indicates time (min) and relative changes in fluorescence (F/F_0) and applies to both traces. (C,D) Summary data showing the mean relative fluorescence (+/- SD) of each treatment in A and B. Addition of 100 μM HEX did not significantly decrease the Ca^{2+} response in ChNs (Wilcoxon matched pairs signed rank test, P=0.0625, n=5). Together, application of 300 μM A-317491 and 100 μM HEX significantly reduced the Ca^{2+} response in ChNs (Wilcoxon matched pairs signed rank test, P=0.0313, n=5) (E) The change in fluorescence during exposure to both A-317491 and HEX significantly exceeded that of each drug on its own (Mann Whitney test, P=0.0303, , n_{HEX}=5, $n_{HEX/A-317491}$=6).

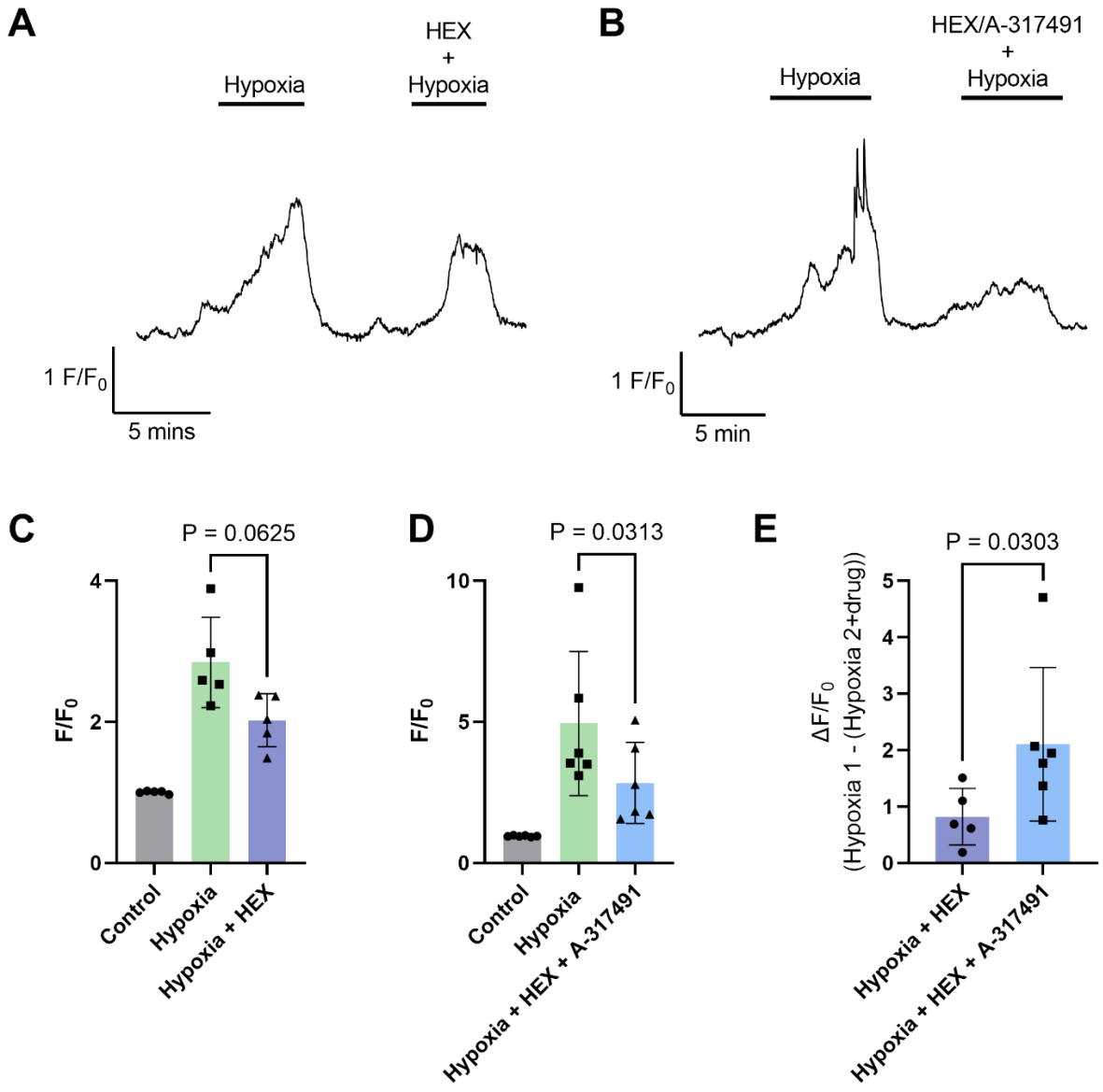
A
HEX
+
Hypoxia
Hypoxia
1 F/F0
5 mins
B
HEX/A-317491
+
Hypoxia
Hypoxia
1 F/F0
5 min
C
P = 0.0625
F/F0
Control
Hypoxia
Hypoxia + HEX
D
P = 0.0313
F/F0
Control
Hypoxia
Hypoxia + HEX + A-317491
E
P = 0.0303
ΔF/F0
(Hypoxia 1 - (Hypoxia 2+drug))
Hypoxia + HEX
Hypoxia + HEX + A-317491

Figure 4

(Fig 4A-C, Fig. 3A). The percent inhibition produced by HEX and A-317491 at their respective IC_{50} values were 28.4% (Fig. 4A) and 35.2% (Fig. 3A), whereas in combination, the hypoxic response was diminished by 46.9% (Fig. 4B, P=0.0303, n_{HEX}=5, $n_{A\text{-}317491}$=6).

A purinergic component of the hypoxic response was detected in vagal sensory ganglia

To assess whether the hypoxic signal, previously detected in the vagal sensory ganglia by Reed *et al.* (2025), also included a purinergic element, a preparation from that study was adapted to assess P2X2/3 receptor activity in the epibranchial ganglia (ebg) and nodose ganglion (ng) of the vagus nerve in 14-21 dpf larvae (Fig 5A,B). A-317491 was used to inhibit P2X2/3 receptors to investigate vagal sensory ganglia (ebg and ng) activity in the head.

The hypoxic response of the ebg and ng decreased upon blockade of P2X2/3 receptors with 300 μM A-317491 during hypoxia exposure. Changes in relative fluorescence indicated a significant decrease in $[Ca^{2+}]_i$ of the ebg and ng when exposed to A-317491 (Fig. 5C-F, P=0.0313, n=6, for both epg and ng).

Adenosine receptor activity was not observed

To investigate a potential role of adenosine receptors in hypoxia signalling in the zebrafish, we used broad spectrum and specific antagonists to attempt to inhibit the ChN $[Ca^{2+}]_i$ response to hypoxia. To begin, 300 μM of the broad-spectrum antagonist caffeine, was applied to the bath during hypoxia and no change in $[Ca^{2+}]_i$ in ChNs was detected when compared to the initial hypoxia exposure (Fig. 6A,B, P>0.9999, n=9). Next, application of 10 μM of the specific A2a antagonist, SCH 58261, was evaluated during hypoxia and no change in $[Ca^{2+}]_i$ was detected in ChNs in comparison to the initial hypoxia exposure (Fig. 6C,D, P>0.9999, n=6)

Figure 5. A-317491 reduced the hypoxic response in vagal sensory ganglia. (A) Fluorescence image of a lateral view of larval zebrafish is shown. Dashed boxes surround the nodose ganglion (ng, purple) and numbered epibranchial ganglia (ebg, blue, 1-4) of the vagus nerve (cranial nerve X). Scale bar represents 0.25 mm. The hindbrain eye and gills are shown for reference. (B) Schematic representation of A. (C) A Ca^{2+}-imaging trace of the ng demonstrates a significant (18.7%) decrease in the $[Ca^{2+}]_i$ response to hypoxia in the presence of 300 μM A-317491. Scale indicates time (min) and relative changes in fluorescence (F/F_0). (D) Summary data of mean relative fluorescence +/- SD associated with each exposure in C (Wilcoxon test, P=0.0313, n=6). (E) A Ca^{2+}-imaging trace of ebg 3-4 demonstrating a significant (18.2%) decrease in the $[Ca^{2+}]_i$ response to hypoxia by 300 μM A-317491. Scale indicates time (min) and relative changes in fluorescence (F/F_0). (F) Summary data of mean relative fluorescence +/- SD associated with each exposure in E (Wilcoxon test, P=0.0313, n=6).

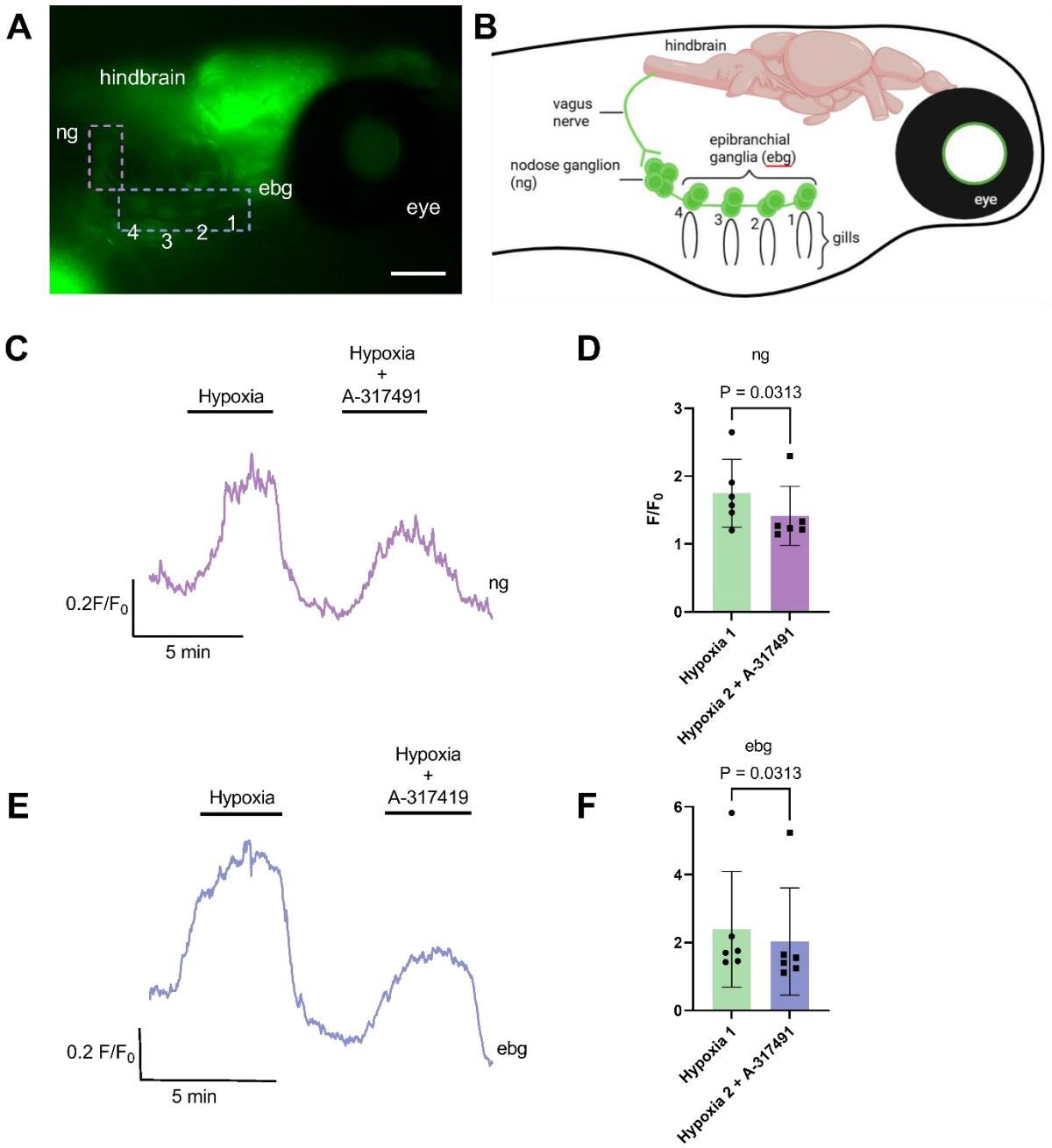
A
hindbrain
ng
ebg
eye
4
3
2
1
B
hindbrain
vagus nerve
nodose ganglion (ng)
epibranchial ganglia (ebg)
eye
gills
C
Hypoxia
Hypoxia + A-317491
0.2F/F0
5 min
ng
D
ng
P = 0.0313
F/F0
Hypoxia 1
Hypoxia 2 + A-317491
E
Hypoxia
Hypoxia + A-317419
0.2 F/F0
5 min
ebg
F
ebg
P = 0.0313
Hypoxia 1
Hypoxia 2 + A-317491

Figure 5

Figure 6. Exposure of gill filaments to adenosine receptor A_{2a} antagonists, caffeine and SCH58261, showed no change in the chain neuron response to hypoxia. (A) A Ca^{2+} -imaging trace showing no change in the $[Ca^{2+}]_i$ response to hypoxia when 300 μM caffeine was present. Scale indicates time (min) and relative changes in fluorescence (F/F_0). (B) Summary data of mean relative fluorescence +/- SD associated with each exposure in A (Friedman test with multiple comparisons, P>0.9999, n=9). (C) A Ca^{2+} -imaging trace showing no change in the $[Ca^{2+}]_i$ response to hypoxia in the presence of 10 μM SCH. Scale indicates time (min) and relative changes in fluorescence (F/F_0). (D) Summary data of mean relative fluorescence +/- SD associated with each exposure in C (Friedman test with multiple comparisons, P>0.9999, n=6).

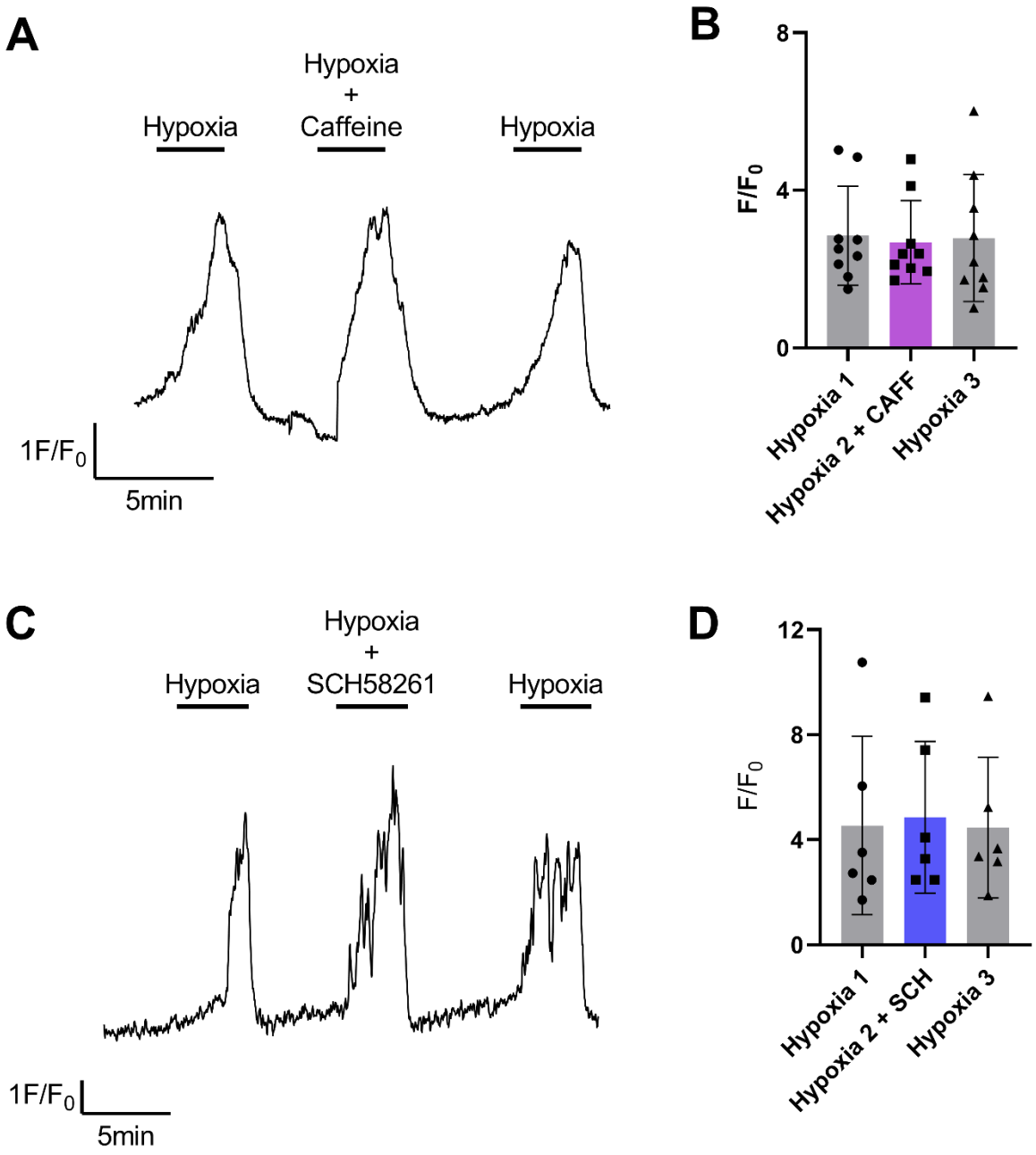
A
Hypoxia
Hypoxia + Caffeine
Hypoxia
1F/F0
5min
B
F/F0
8
4
0
Hypoxia 1
Hypoxia 2 + CAFF
Hypoxia 3
C
Hypoxia
Hypoxia + SCH58261
Hypoxia
1F/F0
5min
D
F/F0
12
8
4
0
Hypoxia 1
Hypoxia 2 + SCH
Hypoxia 3

Figure 6

Next, to determine if adenosine receptors could be detected in the vagal sensory ganglia, larval zebrafish (14-21dp) were exposed to 10 μM of the specific A2a adenosine receptor antagonist, SCH 58261. No significant changes in $[Ca^{2+}]_i$ were detected in the ebg when exposed to SCH 58261 during hypoxia when compared to the first hypoxia exposure (Fig. 7A,B, $P>0.2188$, $n=6$). Similarly, no change in $[Ca^{2+}]_i$ was detected in the ng when exposed to SCH 58261 in the presence of hypoxia in comparison to the first hypoxia exposure (Fig. 7C and D, $P=0.8438$, $n=6$).

Figure 7. Application of SCH 58261 did not change the hypoxic response in vagal sensory ganglia. (A) A Ca^{2+}-imaging trace of the ng demonstrating no significant change in the $[Ca^{2+}]_i$ response to hypoxia in the presence of 10 μM SCH 58261. Scale indicates time (min) and relative changes in fluorescence (F/F_0). Summary data of mean relative fluorescence +/- SD associated with each exposure in A (Wilcoxon test, P=0.2188, n=6). (C) A Ca^{2+}-imaging trace of ebg 3-4 demonstrating no change in the $[Ca^{2+}]_i$ response to hypoxia when 10 μM SCH 58261 was added. Scale indicates time (min) and relative changes in fluorescence (F/F_0). (D) Summary data of mean relative fluorescence +/- SD associated with each exposure in C (Wilcoxon test, P=0.8438, n=6).

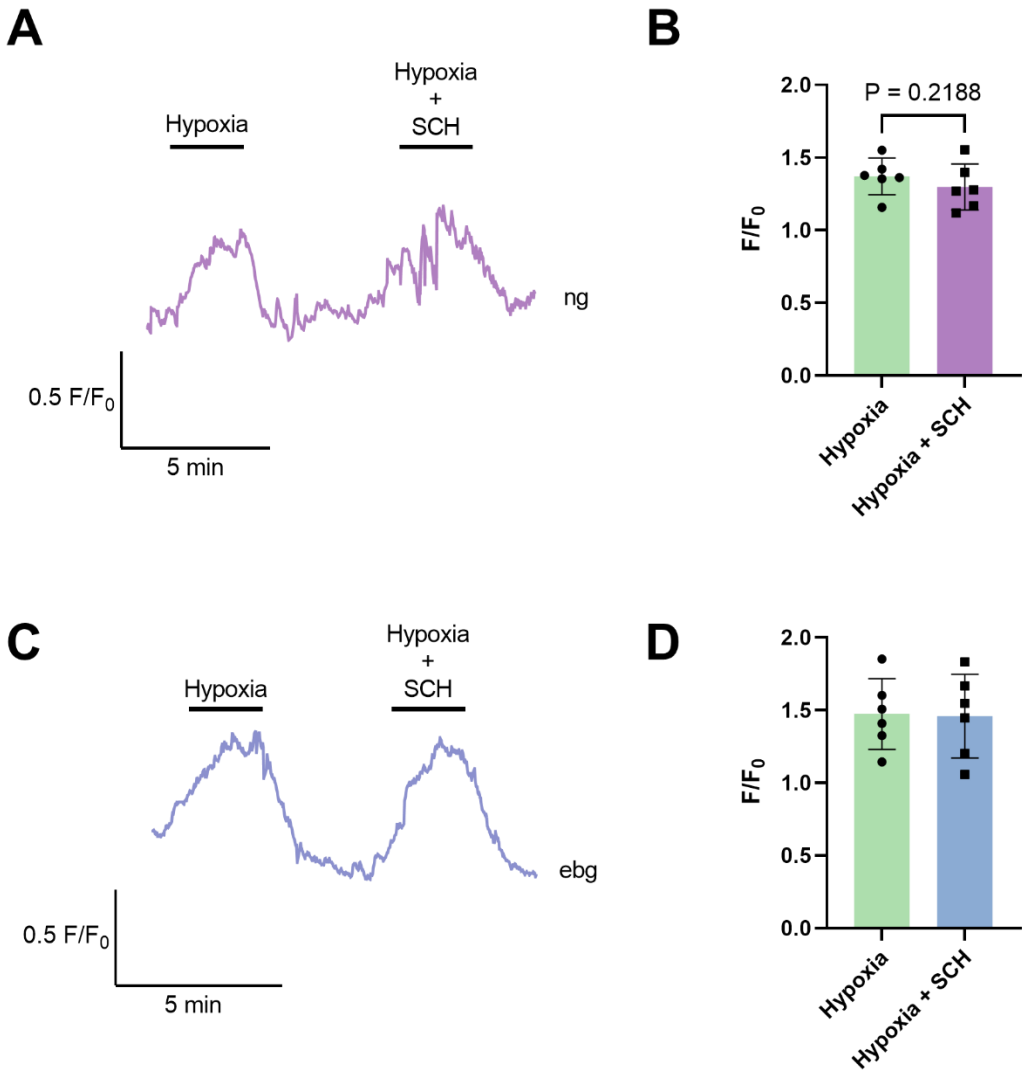
A
Hypoxia
Hypoxia
+
SCH
ng
0.5 F/F0
5 min
B
P = 0.2188
F/F0
2.0
1.5
1.0
0.5
0.0
Hypoxia
Hypoxia + SCH
C
Hypoxia
Hypoxia
+
SCH
ebg
0.5 F/F0
5 min
D
F/F0
2.0
1.5
1.0
0.5
0.0
Hypoxia
Hypoxia + SCH

Figure 7

Discussion

The present study investigated whether purinergic signaling mechanisms are involved in the sensing of hypoxia in the zebrafish gill. It was found that ATP plays a major excitatory role in hypoxia signalling both at the level of the NEC-ChN synapse and the vagal sensory ganglia. Furthermore, it was determined that ATP and ACh target post-synaptic elements in the gill to facilitate hypoxia signalling to the hindbrain.

ATP receptors

ATP plays a major excitatory role in hypoxia signalling in type I cells of the mammalian CB (Zhang *et al.,* 2000). In the zebrafish, a recent study has shown that ACh acts as an excitatory neurotransmitter during a hypoxic event, though the Ca^{2+} response to hypoxia was not fully abolished by the nAChR antagonist, hexamethonium (Reed *et al.,* 2025). This suggested a role for a secondary neurotransmitter also responsible for initiating reflex hyperventilation. We first assessed a role for ATP as a candidate neurotransmitter in hypoxia signaling as it was previously found that agonists an antagonists of purinergic receptors caused changes in ventilation at the whole-animal level in zebrafish (Rahbar *et al*., 2016; Coe *et al.,* 2017). Furthermore, qPCR results showed expression of *p2x2* and *p2x3b* in the zebrafish gill, genes encoding P2X2 and P2X3 purinergic receptors (Reed, 2025) and localization by immunohistochemistry showed receptors present in lamellae (Jonz and Nurse 2003; Rahbar *et al*., 2016).

In the present study, ATPγS, a broad spectrum P2X agonist caused an increase in $[Ca^{2+}]_i$ from the baseline in the absence of hypoxia. This result suggests that exogenously applied ATP, in the absence of hypoxia, mimicked a hypoxic response presumably having an excitatory effect on post-synaptic P2X receptors and implicating purinergic involvement at the level of the ChN.

Furthermore, suramin, a broad-spectrum P2X antagonist caused a decrease in $[Ca^{2+}]_i$ suggesting a partial attenuation of the hypoxic response. This result suggests that exogenously applied suramin blocked the endogenous ATP that would act on P2X receptors, limiting the cellular response to hypoxia at the level of the ChN.

Both results from the above experiments agree with the previous findings that suramin decreased the hyperventilatory response to hypoxia whereas ATPγS stimulated hyperventilation in the absence of hypoxia (Rahbar *et al.,* 2016, Coe *et al.,* 2017). Not only is ATP involved in the hypoxic ventilatory response at the whole-animal level, but the present results indicate that the ATP is released by NECs to act on the purinergic P2 family of receptors post-synaptically and contributes to hypoxia signaling in the zebrafish gill, specifically at the NEC-ChN synapse.

To further characterize ATP signaling in the gill, the specific P2X2/3 antagonist, A-317491, was used. A-317491, applied to the gill during hypoxic exposure, inhibited the change in $[Ca^{2+}]_i$ normally exhibited during a hypoxic exposure. These results suggest that A-317491, exogenously applied, blocked the endogenous ATP from acting on P2X2/3 receptors, limiting the cellular response to hypoxia at the level of the NEC and implicating the specific receptor subtype (P2X2/3) in the ventilatory response to hypoxia. In the mammalian carotid body, ATP has an excitatory post-synaptic effect on P2X2 receptors. Mice lacking the P2X2 receptor exhibit a marked depression in ventilation (Rong *et al.,* 2003). P2X3 receptors of the carotid sinus nerve petrosal ganglion of rats exhibited decreased activity in response to stimulation with A-317491 as well as an overall decrease in ventilation (Niane *et al.,* 2011). Blockade of post-synaptic P2X2/3 receptors by A-317491 in the present study is consistent with the inhibition in ventilation described previously in the zebrafish.

To demonstrate that the hypoxic signal is sent to the hindbrain and that ATP is involved at the level of the vagus nerve, A-317491 was then applied to the whole animal and Ca^{2+}-imaging data was collected from the vagal sensory ganglia. Previous studies have shown that at the level of the vagus nerve, hypoxia caused an increase in $[Ca^{2+}]_i$ at the ebg and the ng in zebrafish and that the response is directional–$[Ca^{2+}]_i$ changes first occur in the gill which is then followed by the ebg and finally the ng (Reed *et al*., 2025). We showed simultaneous recordings from both the ng and ebg of zebrafish aged 14-21dpf indicating a decrease in the $[Ca^{2+}]_i$ response to hypoxia during exposure to A-317491. This attenuation of the response to hypoxia suggests that at the level of the vagus nerve, A-317491 causes inhibition of P2X2/3 receptors further involving P2X2/3 receptors in the modulation of the ventilatory response to hypoxia in higher order neurons.

ATP and ACh are co-released during a hypoxic response

Previous studies showed that during hypoxia, NECs release acetylcholine to act on post-synaptic nAChRs of ChNs (Reed *et al*., 2025). Blockade of nAChRs with hexamethonium showed depression in the hypoxic response in a dose-dependent manner (Reed *et al*., 2025) however, full attenuation of the response remained to be seen. In the mammalian CB, ACh is co-released with ATP from type I cells onto afferent petrosal terminals and together, are largely responsible for signaling during hypoxia exposure (Zhang *et al*., 2000). In the present study, when applied during hypoxia at the IC_{50} of both HEX and A-317491, the decrease in $[Ca^{2+}]_i$ in ChNs exceeded that of each drug individually. This suggests that ATP and ACh are co-released during a hypoxic event to activate the cellular response to hypoxia of post-synaptic ChNs, suggesting their mediation of the ventilation response in zebrafish.

There are many potential mechanisms by which co-release of ATP and ACh may occur in NECs. It can be suggested that the neurotransmitters are stored and released from the same

vesicles, they are stored in separate vesicles but released from the same NEC, or a combination of the above two mechanisms (both neurotransmitters are stored both in the same vesicle as well as in individual vesicles in the same NEC). While all of the above mechanisms are possible, Fig.8 illustrates that ATP and ACh may be stored together as well as separately but released simultaneously to act on post-synaptic ChNs. There are multiple instances of ATP and ACh being co-released across various systems however, the exact storage of the neurotransmitters in vesicles remains uncertain (reviewed in Burnstock, 2020). In the CB, it was proposed that ATP may be stored in cholinergic vesicles of type I cells (Zhang *et al*., 2000). "ATP-induced ATP release" is also a mechanism of ATP release present in the CB, whereby the release of ATP from type 1 cells stimulates further release of ATP via pannexin-1 channels of supporting type 2 cells (Piskuric and Nurse, 2012). This mechanism is also plausible in the zebrafish gill given that ATP is ubiquitous and may be released from supporting cells in the filaments though further research is required. In the marine ray (*Torpedo californica*) single-vesicle imaging of electroplaques showed co-localization across most vesicles, of vesicular nucleotide transporter and vesicular ACh transporter (both necessary for loading of ATP and ACh into vesicles), suggesting ATP and ACh may be stored in the same vesicles (Li and Harlow, 2014). Further, ChNs do not respond directly to stimulation with hypoxia. When the connection between NECs and ChNs was chemically and physically ablated, the Ca^{2+} response was inhibited (Reed and Jonz 2024). This may suggest that ATP is released directly from NECs. The results of the present study suggest that upon cellular activation of NECs during hypoxia, ATP and ACh are released to activate post synaptic P2X2/3 receptors and nAChRs to facilitate hypoxia signaling to the hindbrain however, the exact mechanism is unknown.

Figure 8. Schematic representation of the co-release of ACh and ATP from NECs. The schematic shows ATP (red) and ACh (purple) being released from either the same or individual vesicles of a NEC to act on P2X2/3 receptors and nAChRs of ChN nerve terminals.

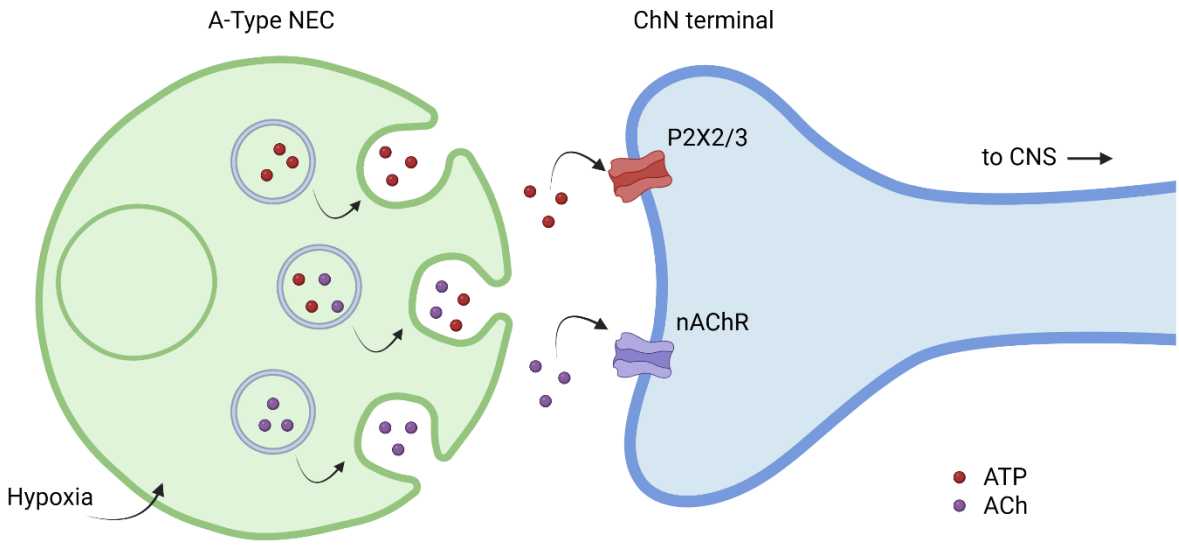

Figure 8

Adenosine receptors

In the mammalian CB, adenosine is believed to have auto/paracrine roles during acute hypoxia. A2a receptors on type I cells are thought to enhance the hypoxic response in the CB through autocrine mechanisms, and A2a receptors are also present post-synaptically (Conde *et al*., 2006). In order to determine whether adenosine plays a role in hypoxia signalling in zebrafish through activation of A2a receptors, we exposed gills and whole-larvae to broad spectrum and specific A2a antagonists.

Results from this study showed that at the level of the NEC-ChN synapse, the broad spectrum P1 antagonist, caffeine, and the specific A2a antagonist, SCH 58261, had no effect on post-synaptic $[Ca^{2+}]_i$ during hypoxia exposure. Furthermore, at the level of the vagus nerve, SCH 58261 had no effect on the $[Ca^{2+}]_i$ of the ebg and ng. Previous studies using zebrafish have shown that both of the above-mentioned drugs were inhibited the hyperventilatory response to hypoxia in juveniles between 14 and 16 dpf (Rahbar *et al.,* 2016; Coe *et al.,* 2017). Furthermore, inhibition of ventilation through aminophylline, a blocker of A1 and A2 adenosine receptors, was noted in both the common carp (*Cyprinus carpio*) and the epaulette shark (*Hemiscyllium ocellatum*, Stenslokken *et al*., 2004; Stecyk and Farrell, 2006). Blockade of A1 and A2 with aminophylline in the common carp also indicated adenosine may be involved in cardiorespiratory control, suggesting its effects on vascular tone (Stecyk and Ferrell, 2006). In the trout, the eFA demonstrated vasoconstriction upon exposure to hypoxia (Sundin and Nilsson, 1997), an effect that was also seen upon exposure to 5-HT and was reversed when exposed to inhibitors of 5-HT receptors (Sundin *et al*., 1998). Adenosine acting on filamentous A1 receptors caused branchial vasoconstriction, an effect that was blocked by the A1 antagonist N6-cyclopentyltheophylline (Sundin and Nilsson, 1996). While it was found that 5-HT acts on extrinsic nerve fibres of higher

order neurons in zebrafish (Reed *et al.,* 2025), it is also proposed that 5-HT is released form NECs to cause vasoconstriction during hypoxia. The present study indicated that adenosine acting through A2a does not excite ChNs nor vagal sensory ganglia, suggesting that adenosine may act elsewhere to mediate the ventilatory response to hypoxia in the zebrafish. A potential hypothesis moving forward is that adenosine may act locally in the zebrafish gill, through A1 and 2Ab receptors, as a vasoconstrictor during hypoxia. Alternatively, hypoxia may act through other adenosine receptors such as A1, A2b or A3 to activate the ventilatory response.

Data collected for the current study used only one single level of severe, acute hypoxia (35 mmHg) to mimic a hypoxic environment. In reality, aquatic vertebrates are generally challenged with varying levels of hypoxia. In studies using the rat CB, Conde *et al* (2006) determined that at moderate levels of hypoxia, adenosine release increased compared to higher levels of hypoxia. This suggests that adenosine release was more relevant at lower levels of hypoxia compared to ATP. The results of the present study show that inhibitors of adenosine receptors have no effect in the gill or vagal sensory ganglia during severe hypoxia, whereas ATP receptors are inhibited at the same level of hypoxia. This suggests, similar to dynamics in the carotid body, the sensitivity of ATP and adenosine to varied levels of hypoxia may differ. Work to expand the role of adenosine in the zebrafish gill should include exposing the preparation to varying levels of hypoxia to create a profile for the contributions of ATP and adenosine at environmentally-relevant levels of O_2.

To date, there is minimal evidence of adenosine receptors in the zebrafish gill. Preliminary work (Reed, 2025) showed mRNA expression of *adora2aa,* the gene encoding adenosine receptor A2a, in the gills of zebrafish increased after a 48-hr exposure to hypoxia though no other P1 receptor mRNA expression was investigated in that study. These data suggest that the A2a receptor is present in the gill but does not localize it to NEC or neuron. Further studies should include qPCR

analysis of P1 receptors to determine their expression in the gill as well as immunohistochemistry to characterize the location of adenosine receptors to specific cell types.

Conclusion

The present study found ATP to play a major excitatory role in the cellular response to hypoxia in zebrafish, implicating it in the initiation of the reflex hyperventilatory response. This work has expanded on the findings at the whole-animal level regarding hypoxia exposure and ventilation. A number of neurotransmitters have been implicated in the ventilatory response to hypoxia and the role they play at the level of the NEC-ChN junction. Recordings of adult gill post-synaptic neurons and vagal sensory ganglia demonstrated changes in $[Ca^{2+}]_i$, suggesting ATP acts on post-synaptic P2X2/3 receptors to mediate reflex hyperventilatory responses to hypoxia. Adenosine receptor antagonists, caffeine and SCH58261, caused no change in $[Ca^{2+}]_i$, at the level of the NEC or vagal sensory ganglia suggesting that adenosine may have local effects on vasoconstriction. Furthermore, it was found that ATP and ACh may be co-released to act post-synaptically suggesting that this mechanism of co-release of neurotransmitters during a hypoxic event is a conserved feature among vertebrates. Studying the mechanism of purinergic signalling involved in the hypoxic response may provide a more complete picture of the HVR in the zebrafish and allow us to further understand the evolution of such a conserved and essential physiological response.

Appendix A: Supplemental Figures

Figure 9. Manual pipetting and DMSO controls. (A) No significant change in $[Ca^{2+}]_i$, was demonstrated when ChNs were exposed to 0.5% DMSO during hypoxia. (B) Summary data of showing no significant change in mean relative fluorescence +/- SD associated with each exposure in A (Friedman test with Dunn's multiple comparisons, P=0.7402, n=6). (C) No increase in $[Ca^{2+}]_i$ when ECS containing 0.5% DMSO is manually added to the bath. (D) Summary data of mean relative fluorescence +/- SD associated with each exposure in C (Friedman test with Dunn's multiple comparisons, P=0.0055, n=6).

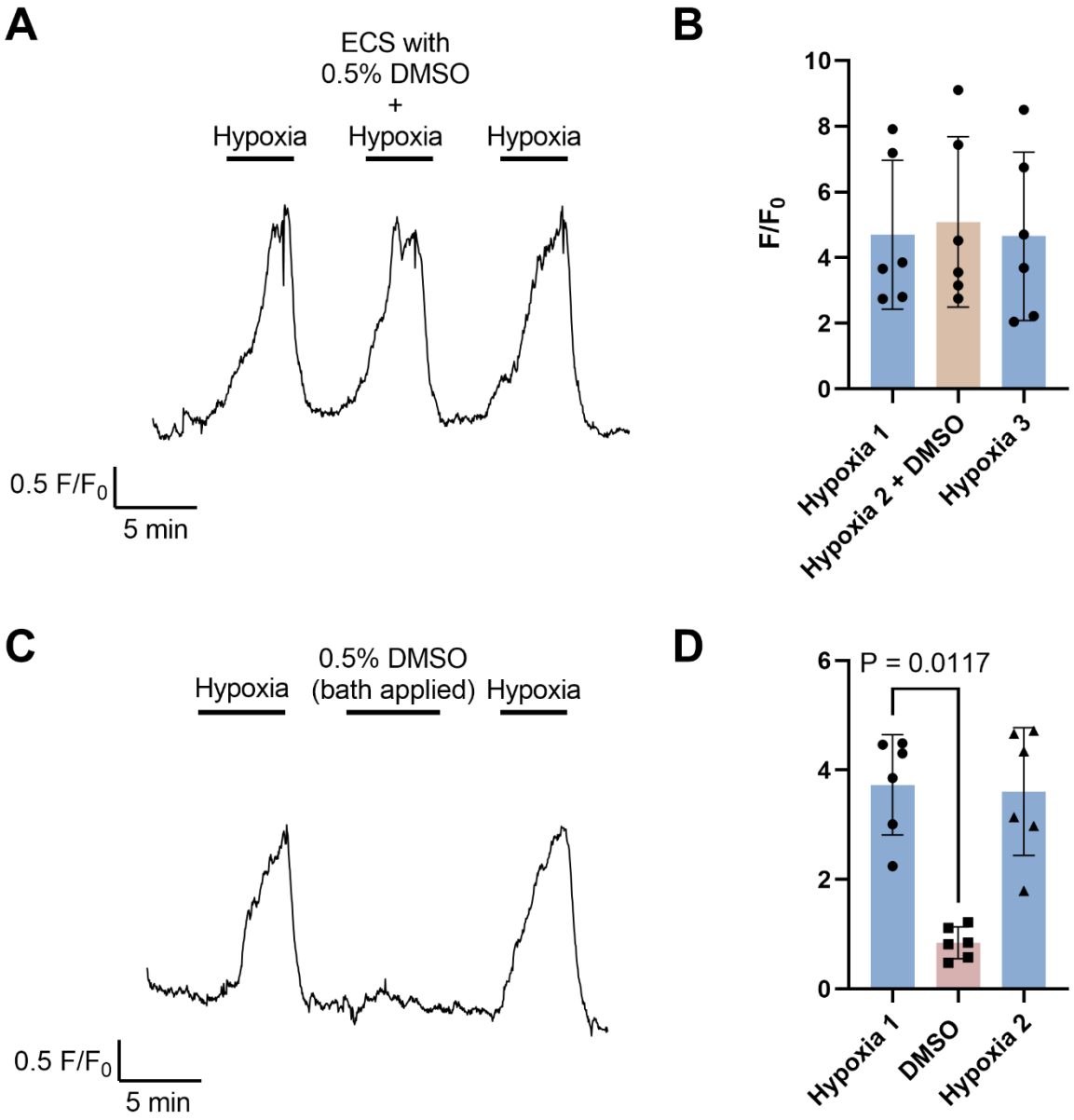
A
ECS with
0.5% DMSO
+
Hypoxia
Hypoxia
Hypoxia
0.5 F/F0
5 min
B
F/F0
10
8
6
4
2
0
Hypoxia 1
Hypoxia 2 + DMSO
Hypoxia 3
C
0.5% DMSO
Hypoxia
(bath applied)
Hypoxia
0.5 F/F0
5 min
D
P = 0.0117
6
4
2
0
Hypoxia 1
DMSO
Hypoxia 2

Figure 9

References

Abdallah, S. J., Jonz, M. G., & Perry, S. F. (2015). Extracellular H+ induces Ca2+ signals in respiratory chemoreceptors of zebrafish. *Pflügers Archiv*, *467*(2), 399–413.

Bradford, C. S., Sun, L., Collodi, P., & Barnes, D. W. (1994). Cell cultures from zebrafish embryos and adult tissues. *J Tiss Cul Metd*, *16*(2), 99–107.

Brouns, I., Adriaensen, D., & Timmermans, J. (2025). The pulmonary neuroepithelial body microenvironment represents an underestimated multimodal component in airway sensory pathways. *Anat. Rec (Hoboken, N.J. : 2007)*, *308*(4), 1094–1117.

Burleson M. L. (2009). Sensory innervation of the Gills: O2-sensitive chemoreceptors and mechanoreceptors. *Acta histochemica*, *111*(3), 196–206.

Burleson, M. L., Smatresk, N. J., & Milsom, W. K. (1992). 7 Afferent Inputs Associated with Cardioventilatory Control in Fish. In *Fish Physiol.* (Vol. 12, pp. 389–426). Elsevier Science & Technology.

Burnstock, G. (2018). Purine and purinergic receptors. *Brain. Neurosci. Adv, 2*, 2398212818817494–2398212818817494.

Burnstock, G. (2020). Introduction to Purinergic Signaling. *Purinergic Signal.*, 1–15.

Coe, A. J., Picard, A. J., & Jonz, M. G. (2017). Purinergic and adenosine receptors contribute to hypoxic hyperventilation in zebrafish (Danio rerio). *Comp. Biochem. Physiol. A, 214*, 50–57.

Conde, S. V., & Monteiro, E. C. (2004). Hypoxia induces adenosine release from the rat carotid body. *J. Neurochem*, *89*(5), 1148–1156.

Conde, S. V., Monteiro, E. C., Hayashida, Y., Gonzalez, C., & Kondo, H. (2006). Profiles for ATP and Adenosine Release at the Carotid Body in Response to O2 Concentrations. *Adv. Exp. Med. Biol.*, *580*, 179–184.

Conde, S. V., Monteiro, E. C., Rigual, R., Obeso, A., & Gonzalez, C. (2012). Hypoxic intensity: a determinant for the contribution of ATP and adenosine to the genesis of carotid body chemosensory activity. *J. Appl. Physiol. (1985)*, *112*(12), 2002–2010.

Dunel-Erb, S., Bailly, Y., & Laurent, P. (1982). Neuroepithelial cells in fish gill primary lamellae. *J Appl Physiol (1985)*, *53*(6), 1342–1353.

Dunn, T. W., Mu, Y., Narayan, S., Randlett, O., Naumann, E. A., Yang, C.-T., Schier, A. F., Freeman, J., Engert, F., & Ahrens, M. B. (2016). Brain-wide mapping of neural activity controlling zebrafish exploratory locomotion. *ELife*, *5*, e12741–e12741.

Gao, L., Moreno-Domínguez, A., Ortega-Sáenz, P., & López-Barneo, J. (2025). The carotid body oxygen sensor. *Curr. Opin. Neurobiol. 92*, Article 103022.

Hockman, D., Burns, A. J., Schlosser, G., Gates, K. P., Jevans, B., Mongera, A., Fisher, S., Unlu, G., Knapik, E. W., Kaufman, C. K., Mosimann, C., Zon, L. I., Lancman, J. J., Dong, P. D. S., Lickert, H., Tucker, A. S., & Baker, C. V. H. (2017). Evolution of the hypoxia-sensitive cells involved in amniote respiratory reflexes. *ELife*, *6*.

Hughes, G. M. (1984). 1 general anatomy of the gills. In *Fish physiol.* (Vol. 10, pp. 1-72). Academic Press.

Jonz, M. G., & Nurse, C. A. (2003). Neuroepithelial cells and associated innervation of the zebrafish gill: A confocal immunofluorescence study. *J Comp Neurol (1911)*, *461*(1), 1–17.

Jonz, M.G., Fearon, I.M., & Nurse, C.A. (2004). Neuroepithelial oxygen chemoreceptors of the zebrafish gill: Zebrafish gill O2chemoreceptors. *J Physiol*, *560*, 737–752.

Jonz, M. G., & Nurse, C. A. (2005). Development of oxygen sensing in the gills of zebrafish. *J Exp Biol*, *208*(Pt 8), 1537–1549.

Laurent P (1984) Gill internal morphology. In: Hoar WS, Randall DJ (eds) *Fish Physiol*. Vol XA, New York, Academic Press, pp 73–183.

Li, H., & Harlow, M. L. (2014). Individual synaptic vesicles from the electroplaque of *Torpedo californica*, a classic cholinergic synapse, also contain transporters for glutamate and ATP. *Physiol. Rep. 2*(1), e00206-n/a.

López-Barneo J, López-López JR, Ureña J, González C. Chemotransduction in the carotid body: K+ current modulated by PO2 in type I chemoreceptor cells. *AAAS*. 1988; 241:580–582.

McQueen, D. S., Bond, S. M., Moores, C., Chessell, I., Humphrey, P. P. A., & Dowd, E. (1998). Activation of P2X receptors for adenosine triphosphate evokes cardiorespiratory reflexes in anaesthetized rats. *J. Physiol. 507*(3), 843–855.

McQueen, D. S., & Ribeiro, J. A. (1983). On the specificity and type of receptor involved in carotid body chemoreceptor activation by adenosine in the cat. *Br. J. Pharmacol. 80*(2), 347–354.

Nakai, J., Ohkura, M. & Imoto, K. A high signal-to-noise Ca^{2+} probe composed of a single green fluorescent protein. *Nat Biotechnol* **19**, 137–141 (2001).

Niane, L. M., Donnelly, D. F., Joseph, V., & Bairam, A. (2011). Ventilatory and carotid body chemoreceptor responses to purinergic P2X receptor antagonists in newborn rats. *J. Appl. Physiol. (1985)*, *110*(1), 83–94.

Nurse, C. A. (2014). Synaptic and paracrine mechanisms at carotid body arterial chemoreceptors. *J. Physiol. 592*(16), 3419–3426.

Nurse, C. A., Buttigieg, J., Brown, S., & Holloway, A. C. (2009). Regulation of Oxygen Sensitivity in Adrenal Chromaffin Cells. *Ann NY Acad Sci*, *1177*(1), 132–139.

Perry, S. F., Jonz, M. G., & Gilmour, K. M. (2009). Chapter 5 Oxygen Sensing And The Hypoxic Ventilatory Response. In *Fish Physiol.* (Vol. 27, pp. 193–253). Elsevier Science & Technology.

Piskuric NA & Nurse CA (2012). Effects of chemostimuli on $[Ca^{2+}]_i$ responses of rat aortic body type I cells and endogenous local neurons: comparison with carotid body cells. *J Physiol* 590, 2121–2135

Prasad M, Fearon IM, Zhang M, Laing M, Vollmer C, Nurse CA. Expression of P2X2 and P2X3 receptor subunits in rat carotid body afferent neurones: role in chemosensory signalling. *J Physiol*. 2001 Dec 15;537(Pt 3):667-77. doi: 10.1111/j.1469-7793.2001.

Qin, Z., Lewis, J. E., & Perry, S. F. (2010). Zebrafish (Danio rerio) gill neuroepithelial cells are sensitive chemoreceptors for environmental CO2. *J Physiol*, *588*(5), 861–872.

Rahbar, S., Pan, W., Jonz, M.G. (2016). Purinergic and Cholinergic Drugs Mediate Hyperventilation in Zebrafish: Evidence from a Novel Chemical Screen. *PLoS One*. 11(4):e015261.

Reed, M., & Jonz, M. G. (2025). Oxygen chemoreceptor inhibition by dopamine D2 receptors in isolated zebrafish gills. *J. Physiol. 603*(8), 2369–2385.

Reed, M., Mavridis, A.A., Mennigen, J.A. and Jonz, M.G. (2025), Dual cholinergic and serotonergic excitatory pathways mediate oxygen sensing in the zebrafish gill. *J Physiol*. https://doi.org/10.1113/JP289409

Rombough, P. (2002). Gills are needed for ionoregulation before they are needed for O2 uptake in developing zebrafish, Danio rerio. *J. Exp. Biol*, *205*(12), 1787–1794.

Rombough, P. (2007). The functional ontogeny of the teleost gill: Which comes first, gas or ion exchange? *Comp Biochem Phys A*, *148*(4), 732–742.

Rong, W., Gourine, A. V., Cockayne, D. A., Xiang, Z., Ford, A. P. D. W., Spyer, K. M., & Burnstock, G. (2003). Pivotal Role of Nucleotide P2X2 Receptor Subunit of the ATP-Gated Ion Channel Mediating Ventilatory Responses to Hypoxia. *J.Neurosci. 23*(36), 11315–11321.

Stensløkken, K-O., Sundin, L., Renshaw, G. M. C., Nilsson, G. E. (2004) Adenosinergic and cholinergic control mechanisms during hypoxia in the epaulette shark (*Hemiscyllium ocellatum*), with emphasis on branchial circulation. *J Exp Biol* 1 207 (25): 4451–4461.

Stecyk, J. A. W., & Farrell, A. P. (2006). Regulation of the Cardiorespiratory System of Common Carp (*Cyprinus carpio*) during Severe Hypoxia at Three Seasonal Acclimation Temperatures. *Physiol. Biochem. Zool. 79*(3), 614–627.

Sundin L, Davison W, Forster M, Axelsson M (1998a) A role of 5-HT2 receptors in the gill vasculature of the antarctic fish *Pagothenia borchgrevinki*. *J Exp Biol* 201:2129–2138

Sundin, L., & Nilsson, G. E. (1996). Branchial and systemic roles of adenosine receptors in rainbow trout: an in vivo microscopy study. *Am. J. Physiol. Regul, Integr. Comp. Physiol. 40*(3), R661–R669.

Sundin L, Nilsson GE (1997) Neurochemical mechanisms behind gill microcirculatory responses to hypoxia in trout: in vivo microscopy study. *Am J Physiol Regul Integr Compar Physiol*. 272:R576–R585

Weir, E. K., López-Barneo, J., Buckler, K. J., & Archer, S. L. (2005). Acute Oxygen-Sensing Mechanisms. *N Engl J Med*, *353*(19), 2042–2055.

Westerfield, M. (2000). The zebrafish book. A guide for the laboratory use of zebrafish (Danio rerio). 4th ed., Univ. of Oregon Press, Eugene

Wilson, J.M. and Laurent, P. (2002), Fish gill morphology: inside out. *J. Exp. Zool*., 293:192-213.

Zhang, M., Zhong, H., Vollmer, C., & Nurse, C. A. (2000). Co-release of ATP and ACh mediates hypoxic signalling at rat carotid body chemoreceptors. *J. of Physiol. 525*(1), 143–158.

Zhong, H., & Nurse, C. A. (1997). Nicotinic acetylcholine sensitivity of rat petrosal sensory neurons in dissociated cell culture. *Brain Res. 766*(1), 153–161.